

■ C O R R O S I O N E ■

Corrosion Resistance of Cr (III) Based Conversion Layer on Zinc Coatings in Comparison with a Traditional Cr (VI) Based Passivation Treatment

L. Grasso, A. Segre Fantoli, M. G. Ienco, A. Parodi, M. R. Pinasco, E. Angelini, F. Rosalbino

Industrial hot dip galvanized steels were submitted to a Cr(III)-based passivation treatment (containing phosphates) leading to Cr(VI)-free conversion layers.

The characterization of the substrate and of the coatings was carried out before and after the passivation treatment by means of optical microscopy (OM) and scanning electron microscopy with energy X-ray dispersive spectrometry associated (SEM/EDS). In particular the zinc coating was preliminarily studied both superficially and in section in order to define its adequacy and its possible state of defectiveness.

The corrosion behaviour was evaluated by means of electrochemical impedance spectroscopy (EIS) and salt spray test. A comparison between the protective effectiveness of the innovative Cr(III)-based passivation and the Cr(VI)-based process usually employed by manufacturers was carried out.

According to the exposed preliminary results, promising outcomes were obtained with the innovative Cr(III)-based passivation by optimizing the amount of chromium in the coating.

Key words: chromium alternative passivation treatments, hot dip galvanized steel, salt spray, EIS, SEM/EDS

INTRODUCTION

In the last 20 years, a remarkable development of the zinc plating processes has been observed because of the increasing request from building industry, household appliances and automotive industry for coatings with higher corrosion resistance.

It is well-known that the corrosion resistance of pure zinc coatings may be improved by means of suitable chemical passivation treatments, performed usually by immersion of the zinc coated objects in baths containing chromic acid or an acid solution of Cr(VI) salts. Chromate passivation baths also contain "activators" as fluorides, sulphates, acetates, etc., which increase the thickness of the passivation layer [1]. Various complex reaction schemes have been proposed for the chromating process, but simplifying the formation of the chromate conversion coating is usually described as a red-ox reaction between the oxidising Cr(VI) ions and the metallic substrate [2-3]. The passivation layer is mainly constituted by zinc oxides and hydroxides, zinc chromates, mixed Cr(III) and Cr (VI) oxides and hydroxides. These layers protect the zinc coating by forming a physical barrier between the metal substrate and the corrosive medium [4-5]. In the passivation coating, chromium is present as Cr (III) and Cr (VI). Some studies [6] underline the active role of

soluble Cr (VI) species in increasing the corrosion resistance, and the dependence of the corrosion protection effectiveness on the amount of Cr(VI) within or adsorbed onto the coating after the passivation process.

In the European Community, the use of Cr (VI) compounds, considered a cancer-producing agent, must be withdrawn within a short time, according to the directive 2002/95/CE 27-01-2003. Molybdates, permanganates, vanadates, titanates, rare earth metals and Cr(III) compounds are proposed as alternatives.

Cr(III)-based conversion treatments are extensively studied, because they are considered to be commercially acceptable alternatives to conventional Cr(VI) passivation treatments for several applications [7]. Barnes et al. [8] studied a Cr(III) based process for zinc passivation, containing nitrate as an oxidant and sodium hypophosphite as a complexant to enhance the stability of Cr(III) in the treatment bath. As the conventional chromate conversion coatings, this Cr (III)-based process involves a red-ox reaction between the zinc surface, that is oxidised, and the oxidising agent suffering a reduction. This process brings about a localised pH increase and makes possible the precipitation of insoluble trivalent chromium hydroxide. The colour and the thickness of Cr(III) passivation coating may be modified by changing different parameters as solution composition, pH, temperature and immersion time.

In order to find applicable alternatives to Cr (VI)-based conversion baths, it is of outstanding importance the find cheap coatings processes with good protective effectiveness against corrosion, environmentally friendly and easy to employ in an industrial plant.

In this work industrial hot dip galvanized steels were submitted to a Cr(III) based passivation treatment (containing phosphates and fluorides) leading to Cr(VI)-free conversion layers, characterized from a microchemical, micromorphological and electrochemical point of view.

Also the aesthetic appearance of the artefact has been taken into account, it is of outstanding importance that the surface

L. Grasso, A. Segre Fantoli
ILVA S.p.A., Genova, Italia

M. G. Ienco, A. Parodi, M. R. Pinasco
Università di Genova, Dipartimento di Chimica,
Via Dodecaneso 31, 16046 Genova, Italy

E. Angelini, F. Rosalbino
Politecnico di Torino, Dipartimento di Scienza dei Materiali ed Ingegneria Chimica,
Corso Duca degli Abruzzi 24, 10129 Torino, Italy

Paper presented at the 2nd International Conference
HEAT TREATMENT AND SURFACE ENGINEERING IN AUTOMOTIVE APPLICATIONS
organised by AIM, Riva del Garda, 20-22 June 2005

layer remains shiny with spangle appearance, so the passivation treatment has not to be responsible of darkening phenomena.

For comparison purposes, the performances of coatings industrially produced by means of a traditional Cr(VI)-based passivation treatment were examined.

EXPERIMENTAL

The substrates employed are sheets of hot dip galvanized steels (0.38-1.00 mm thick, respectively code Z1 and Z2) of the Società Ilva S.p.A., Genova. The Zn deposition has been performed on-line by immersion in a melted zinc bath with Al (≤ 0.25 wt%) and Sb (≤ 0.065 wt%).

A series of specimens (Code G) has been submitted to a passivation treatment by means of a Cr(III) based product, in the laboratories of a manufacturer leader in the field. The treatment has been carried out at room temperature with a laboratory Chemcoater followed by a drying step of 10 s at $T=80^{\circ}\text{C}$. Different layers have been obtained by varying the roll pressure of the Chemcoater.

Another series of specimens (Code ZP) has been submitted to a traditional passivation treatment with a chromic acid solution by spraying application, stripping and air.

The amount of Zn (g/m^2) in the layer has been determined on both the surfaces of the specimens by weight loss evaluation before and after washing in hydrochloric acid.

The thickness of the layer has been evaluated on both the surfaces from the deposited amount, taking into account that $\text{density}=\text{mass}/\text{volume}$, and by means of the image analysis on metallographically polished cross-sections.

By means of atomic absorption spectrometry (AAS) the amount of chromium (mg/m^2) in the passivation layers has been determined.

The corrosion resistance has been evaluated on the hot dip galvanized steels before and after the passivation treatments by means of salt spray test and electrochemical impedance spectroscopy (EIS).

Salt spray exposure has been carried out according to ASTM B117 (9) with a sodium chloride solution (5 ± 1 wt%), pH in the range 6.5-7.2, at $T=35^{\circ}\text{C}$. Visual assessments of surface degradation has been performed by evaluating, by image analysis, the percentage of the surface covered by the *white rust* every 24h of exposure, till a coverage of 80%; the maximum exposure time was 96h.

The electrochemical impedance (EIS) measurements have

been carried out at 25°C in NaCl 0.1 M aerated solution. The samples surface exposed to the aggressive environment was 13 cm^2 . The spectra have been recorded at the free corrosion potential, by applying a sinusoidal signal of 10 mV in amplitude and frequency ranging between $100\text{ kHz} \pm 10\text{ mHz}$.

Before and after the passivation treatments and before and after the corrosion tests, the samples have been submitted to microchemical and micromorphological characterization, by means of optical microscopy (OM) and scanning electron microscopy with energy X-ray dispersive spectrometry associated (SEM+EDS).

RESULTS

Microchemical and micromorphological characterization

Hot dip galvanized steel (Code Z)

The surface of all samples appears shiny and shows the typical spangle finish of the zinc coatings; with coarse grains different in size and brightness. The optical micrograph of Fig.1 shows the different solidification morphologies of the grains: one with a rough appearance and dull, others feather-like and shiny. These different morphologies may be explained by taking into account parallel or non parallel growth with respect to the substrate and the presence of secondary dendrites [10]. The dendrites grow parallel to the strip in the shiny feather-like grains. Fig.2 shows a solidification structure with a honeycomb appearance, since the tips of the dendrites grow toward the coating surface. The orthogonal-dendritic morphology is characterized by secondary dendritic arms, which lie at 90° with respect to the area of origin. By means of the EDS microanalysis the surface chemical composition of the different surface layers has been determined as shown in Table 1. The coating is mainly constituted by zinc and by low amounts of Al $< 1\%$, while Sb has never been detected uniformly distributed. The Fe signal may be attributed to the bulk underlying and, as expected, decreases with increasing the coating thickness.

On the surface, inside the grains with the orthogonal-dendritic morphology, aluminium and antimony infradendritic microsegregation was detected by SEM/EDS, see Table 2. No Sb is detected in the axial zone, while it reaches concentrations ranging from 1 to 2% in the infradendritic zones. Al microsegregation occurs at a lower extent, this element reaches concentrations of 1-2% in the infradendritic zones and

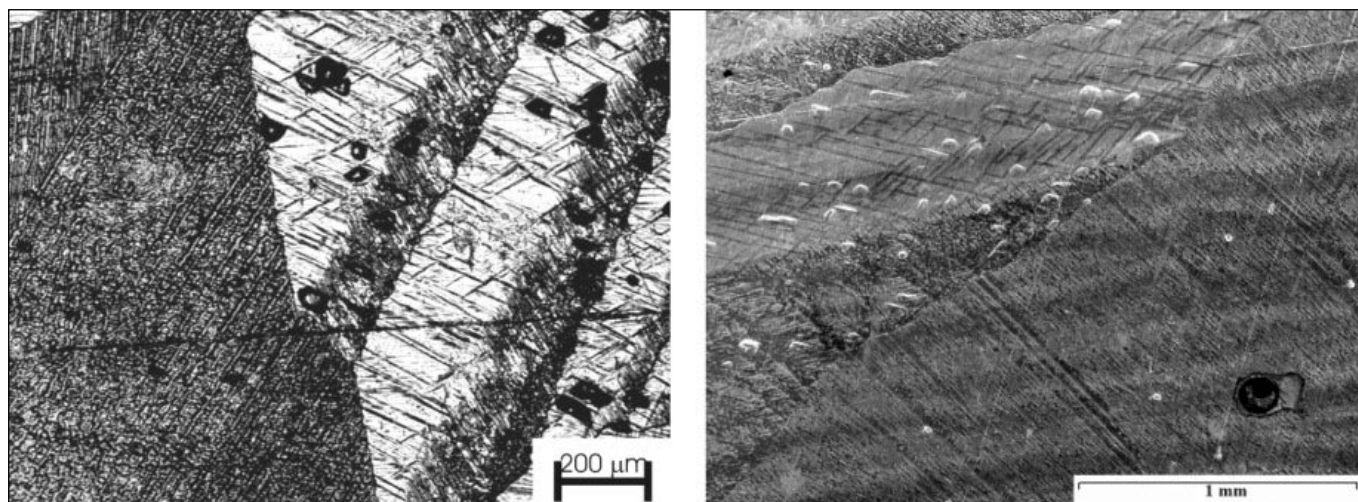


Fig. 1 – Optical image (left) and SEM/SE image (right) of the surface of a Z specimen : grains with different morphology.

Fig. 1 – Immagine ottica (sinistra) e immagine SEM/SE (destra) della superficie di un campione Z, grani cristallini con morfologia differente.

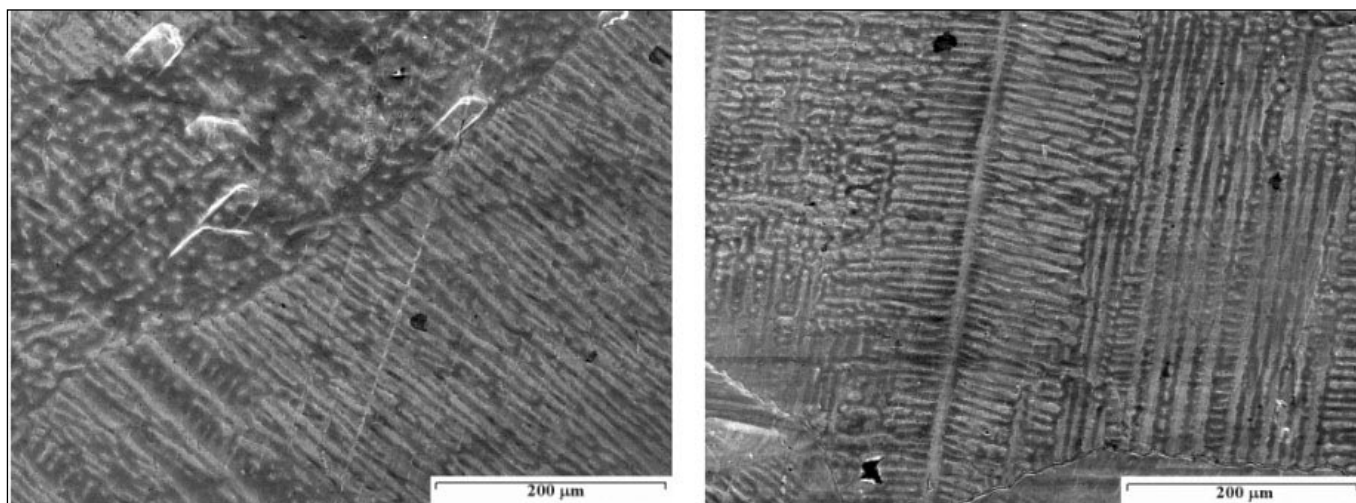


Fig. 2 – SEM/SE image of grains of the surface of a Z specimen with different morphology (left); SEM/SE image showing morphology with orthogonal dendrites (right).

Fig. 2 – Immagine SEM/SE di grani cristallini con morfologia differente della superficie di un campione Z (sinistra) e immagine SEM/SE che mostra la morfologia con dendriti ortogonali (destra).

Code	O	Al	Fe	Zn	Sb	Cr	P	others
Z1	1	1	1-2	97	-	-	-	-
Z2	1	<1	≤1	98	-	-	-	-
ZP4	1	-	<1	98	-	-	-	-
ZP5	2	0-<1	1-2	96	-	-	-	-
ZP6	1-2	1-2	<<1	95-97	0-1	-	-	-
ZP9	3-4	0-<1	<1-1	94-96	-	0-<<1	-	-
G3/b	16	<1	<1	78	-	1	3	<1

Table 1 – Average surface composition (wt %) of the coatings determined by EDS.

Tabella 1 – Composizione media della superficie (% in peso) dello strato determinata con EDS.

Zone	Al	Fe	Zn	Sb
Axial	<1 (0-0.7)	<<1 (0-0.5)	99	0
Infradendritic	1-2	<<1 (0-0.5)	95-97	1-3

Table 2 – EDS analysis of the axial and infradendritic zones in a grain with orthogonal-dendritic morphology of a Z specimen.

Tabella 2 – Analisi EDS delle zone assiali ed infradendritiche di un grano con morfologia dendritica ortogonale di un campione Z.

Code	Zn amount (g/m ²) and Zn thickness (μm) in ZP specimens.	Zn amount (g/m ²) Surface A	Zn thickness (μm)	Zn thickness Image analysis (μm)	Zn amount (g/m ²) Surface B	Zn thickness (μm)	Zn thickness Image analysis (μm)
	ZP1	75	10.5	12.4±1.5	60	8.4	6.4±0.8
ZP2	75	10.5	11.2±1.1	60	8.4	8.1±0.6	
ZP3	60	8.4	7.1±1.1	90	12.6	12.4±0.9	
ZP4	75	10.5	11.1±0.9	75	10.5	11.7±0.5	
ZP5	90	12.6	9.1±0.7	75	10.5	9.7±0.4	
ZP6	90	12.6	15.8±1.5	120	16.8	18.9±0.7	
ZP7	75	10.5	11.4±0.6	60	8.4	8.5±0.5	
ZP8	120	16.8	14.1±0.3	75	10.5	9.4±0.7	
ZP9	90	12.6	13.5±0.7	90	12.6	11.4±0.6	
ZP10	75	10.5	14.0±0.7	60	8.4	9.1±1.0	

Table 3 – Zn amount (g/m²) and Zn thickness (μm) in ZP specimens.

Tabella 3 – Contenuto di Zn (g/m²) e spessore (μm) dello strato di zinco nei campioni ZP.

is also present in the axial zone with amounts < 1%.

The large irregular grains show in different specimens a wide range of dimensions. The number of grains per cm² ranges from 9 to 46; no relationship has been found with the alloying elements content.

Noteworthy differences have been detected on the two surfaces of the same specimen, thus suggesting a noteworthy influence of the process parameters (production rate, cooling rate, etc.).

Cr (VI)-based passivated hot dip galvanized steel (Code ZP)

As shown in Table 3, the overall zinc content (surface A+B) is different for the different specimens, the zinc amount among the two faces ranges from 15 to 45 g/m².

The thickness of the zinc coating, evaluated from the amount deposited per m², ranges from 8.4 to 16.8 μm, the maximum difference among the two faces is 6.3 μm. The zinc thickness evaluated with the image analysis is generally in good accordance with the one obtained from the weight loss measurements.

The chromium content in the passivation layer ranges from 5 to 21 mg/m², as shown in Table 4. A difference has also been observed between the two surfaces (Δ_{max} = 13 mg/m²) of the same specimen. The Cr deposition is maintained to a low extent for aesthetical reasons, because by increasing the ch-

Code	Surface A	Surface B
ZP1	11	7
ZP2	6	9
ZP3	8	6
ZP4	12	10
ZP5	5	6
ZP6	9	8
ZP7	6	7
ZP8	8	7
ZP9	8	21
ZP10	11	9

Table 4 – Chromium content (mg/m²) in the passivation layer determined by AAS.

Tabella 4 – Contenuto di Cromo (mg/m²) nello strato di passivazione determinato mediante AAS.

romium amount in the traditional passivation treatment, the coating darkens.

The surface of the ZP specimens remain shiny, the passivation treatment does not induce great modifications, as shown in the optical microscopy of Fig.3. The SEM observation shows that the passivated surface is uniform and defectless; the spangle morphology is well observed, a slight attack evidences lamellar features inside the grains with dimpled and feather morphology, Fig. 4.

By means of EDS analysis, it may be observed that they are richer in Sb and Al with respect to the matrix (Al 1-2 vs 0- <1 and Sb 1-3 vs 0). Seldom a deeper attack may be observed near the areas in which Sb and Al reach values of 7-4%. In some cases the corrosion attack is localized, as shown in Fig. 4. If the average EDS analysis of the surface layer of ZP specimens is compared with the ones of the Z specimens, the presence of Cr is not evidenced except on ZP9 sample characterized by a high Cr content (21 mg/m² vs 6-10 mg/m²). The oxygen content is highly increased by the passivation treatment, also in this case the element content is higher on the ZP9 specimen, where the zinc content is slightly lower with respect to the other ZP samples. Dealing with the other elements there are not great differences, only on ZP6 sample Sb has been detected together with a high Al content.

Cr(III)-based passivated hot dip galvanized steel (Code G)

The hot dip galvanized steel specimens have been submitted to the Cr(III)-based passivation treatment in different conditions in order to obtain two different Cr contents in the surface layer (20 mg/m² for samples G1/a, G2/a, G3/a and 38 mg/m² for samples G1/b, G2/b, G3/b).

After the passivation treatment the surface of the G samples remains shiny as the one of Z specimens.

The SEM micrographs of Figg.5 and 6 show the different

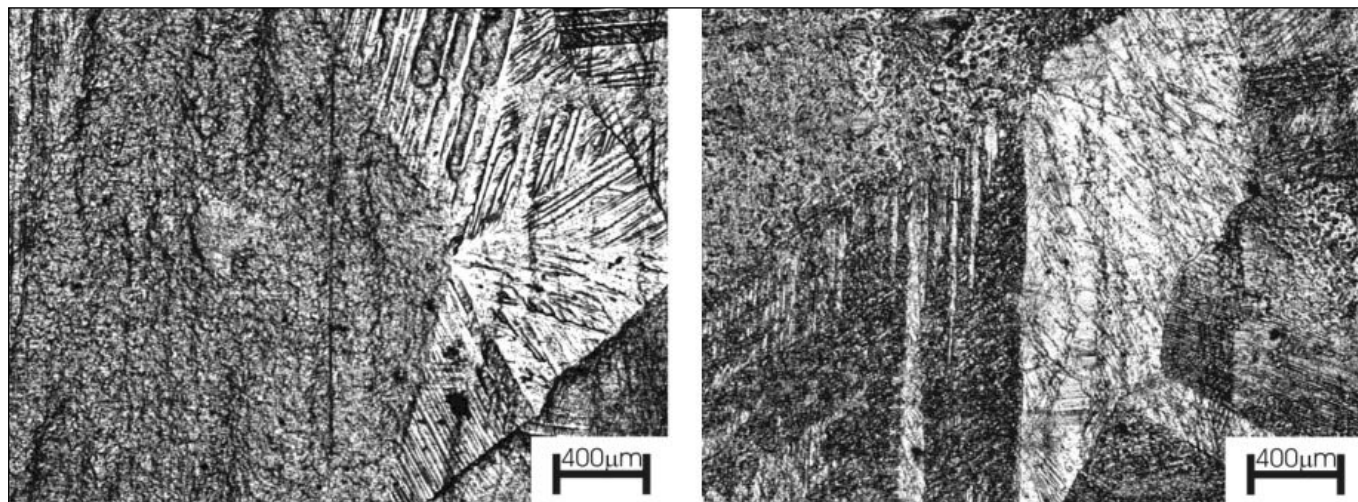


Fig. 3 – Optical images of the surface of a ZP specimen: grains with different morphology.

Fig. 3 – Immagini ottiche della superficie di un campione ZP, grani cristallini con morfologia differente.

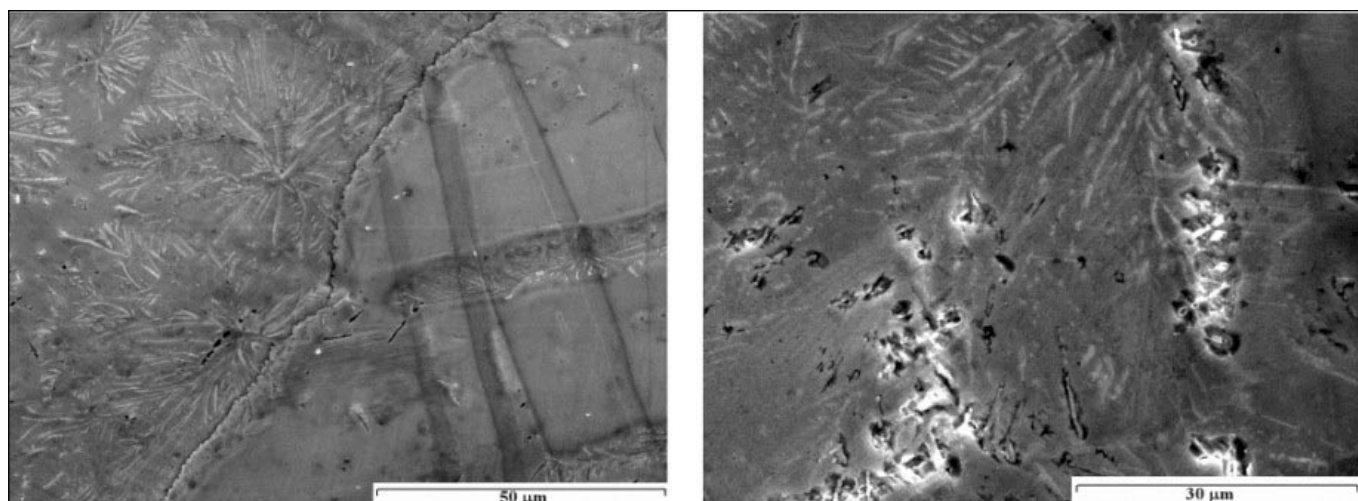


Fig. 4 – SEM/SE images of the surface of a ZP specimen. Lamellar features in dimpled and feather grains (left); localized attack (right).

Fig. 4 – Immagini SEM/SE della superficie di un campione ZP. Zone ad apparenza lamellare situate nei grani con morfologia dimpled e feather (sinistra); attacco localizzato(destra).

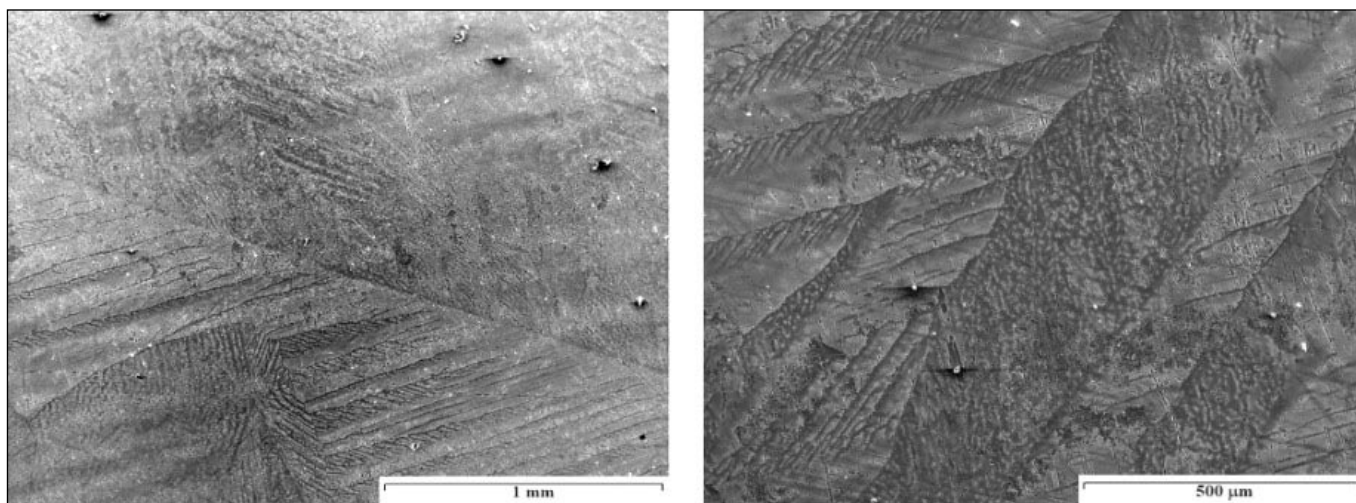


Fig. 5 – SEM/SE images of the surface of a G specimen. Different grain morphologies well evidenced.

Fig. 5 – Immagini SEM/SE della superficie di un campione G. Morfologie differenti ben evidenti nei grani cristallini.

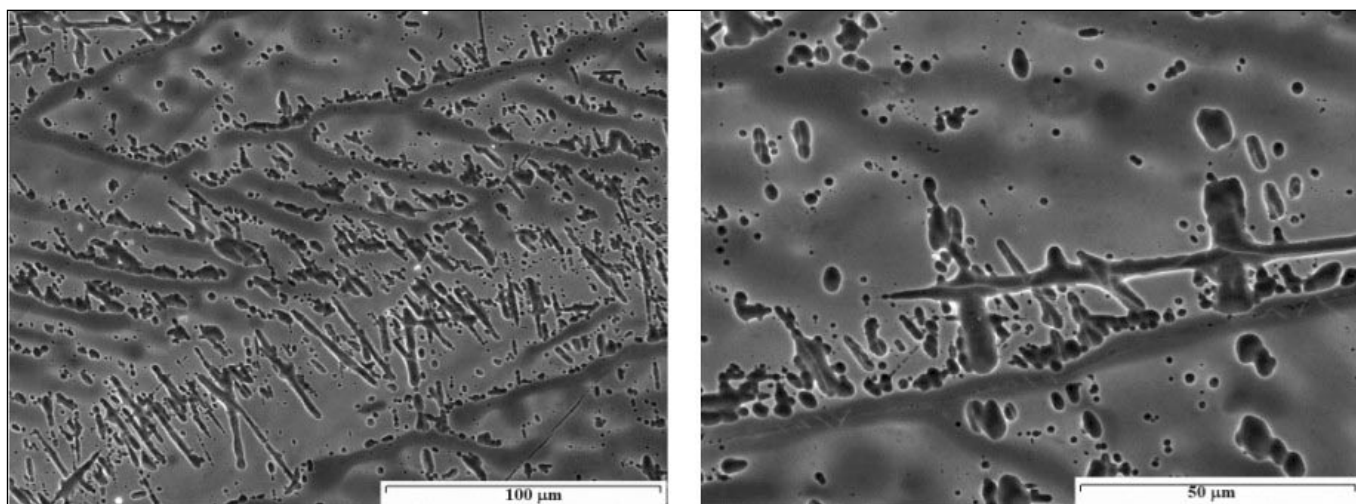


Fig. 6 – SEM/SE images of the surface of a G specimen. Dendritic segregation in relation to the topography and morphology of localized attack.

Fig. 6 – Immagini SEM/SE della superficie di un campione G. Segregazioni dendritiche in relazione alla topografia ed alla morfologia dell'attacco localizzato.

morphologies of the grains and the dendritic segregation in relation to the corrosive attack due to the passivation treatment. The leaves-like grains are extended in elongated areas, in which are evident the dendritic segregations alternated at lighter zones without any segregation: the attack causes the formation of porosities mainly localized in the areas of the grain where the segregation and/or in the dendritic arms, lighter zones, richer in zinc. The porosities show a globular-shape in the axial areas of the dendrites, as shown in Fig. 6 and have an acicular shape with a preferential orientation in the lighter zones of the leaves-like grains.

Fig. 7 shows a part of the surface where attached areas near the infradendritic zones and the composition profile may be observed. An increase of oxygen and phosphorus, and, to a lower extent, of chromium, in the corroded zones has been detected, while Sb and Al are concentrated in the infradendritic zones as shown for Z specimens. On the surface some areas more deeply attacked may be observed, Fig. 8; in these zones, an increase of the oxygen content (26 vs 10-15 %), of phosphorus (5 vs 1-2 %) and chromium (1.5 vs 0.6 %) is observed with respect to the areas nearby less attacked.

Also other elements are present in amounts lower than 1% uniformly distributed in the various zones: Fe is always lower than 1% and its content is lower in the corroded zo-

nes, where Zn decreases from 85 to 65 %. Al < 1% is detected only in the more corroded areas.

The average surface analysis evidences in addition to oxygen, zinc, iron and aluminium also the presence of chromium and phosphorus, see Table 1. In comparison with ZP specimens a higher O and Cr content and a lower Zn content is detected.

Corrosion resistance evaluation

Salt spray test

The salt spray test has been carried out on a series of ZP and G specimens. In Table 5 the percentage of the corroded surface at increasing exposure times may be observed.

The hot dip galvanized steel (code Z2), after 24h of exposure, is uniformly corroded, almost 80% of the surface is covered by a layer of *white rust*, essentially zinc hydroxide, few areas uniformly distributed are still shiny.

Almost all the ZP samples, in the exposure range 48-96h, corrode to a noteworthy extent, more than 80% of the surface covers with a layer of white corrosion products. At the end of the test, the surface of ZP specimens is similar to the one of Z samples after 24 h of exposure: the corrosion attack is uniform and the coverage of the surface is almost complete also if few

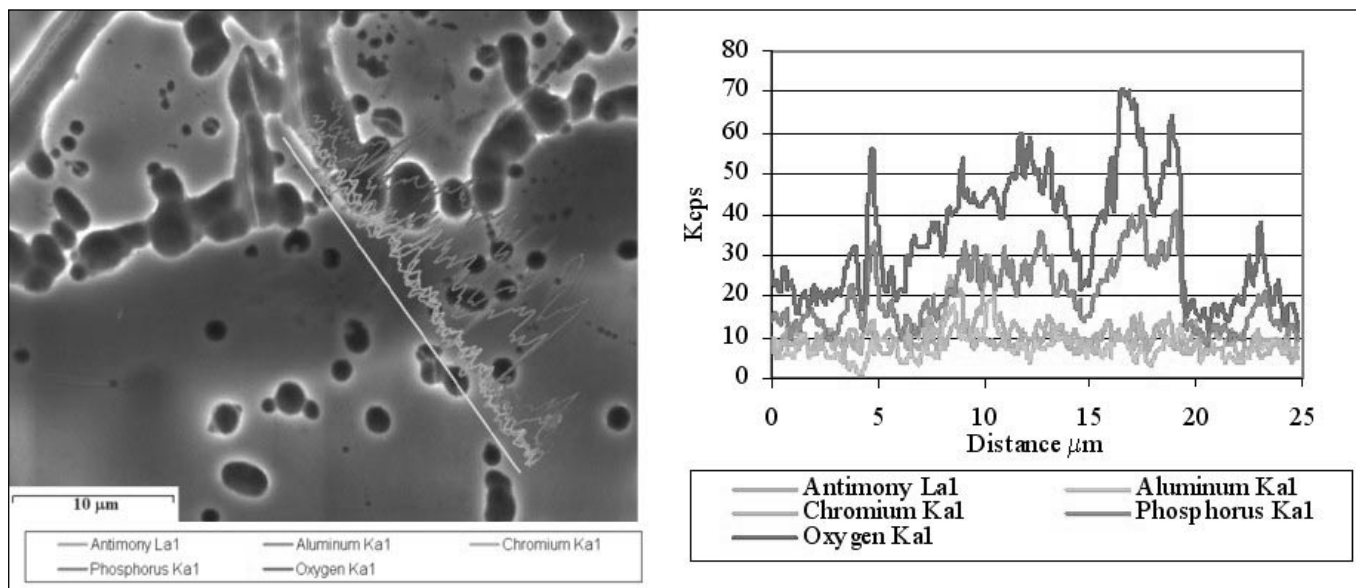


Fig. 7 – SEM/SE image of the surface of a G specimen: preferential attack areas are evidenced together with infradendritic zones; EDS composition profiles for various elements.

Fig. 7 – Immagini SEM/SE della superficie di un campione G: sono evidenziate aree di attacco preferenziale assieme alle zone infradendritiche; profili di composizione EDS per i vari elementi.

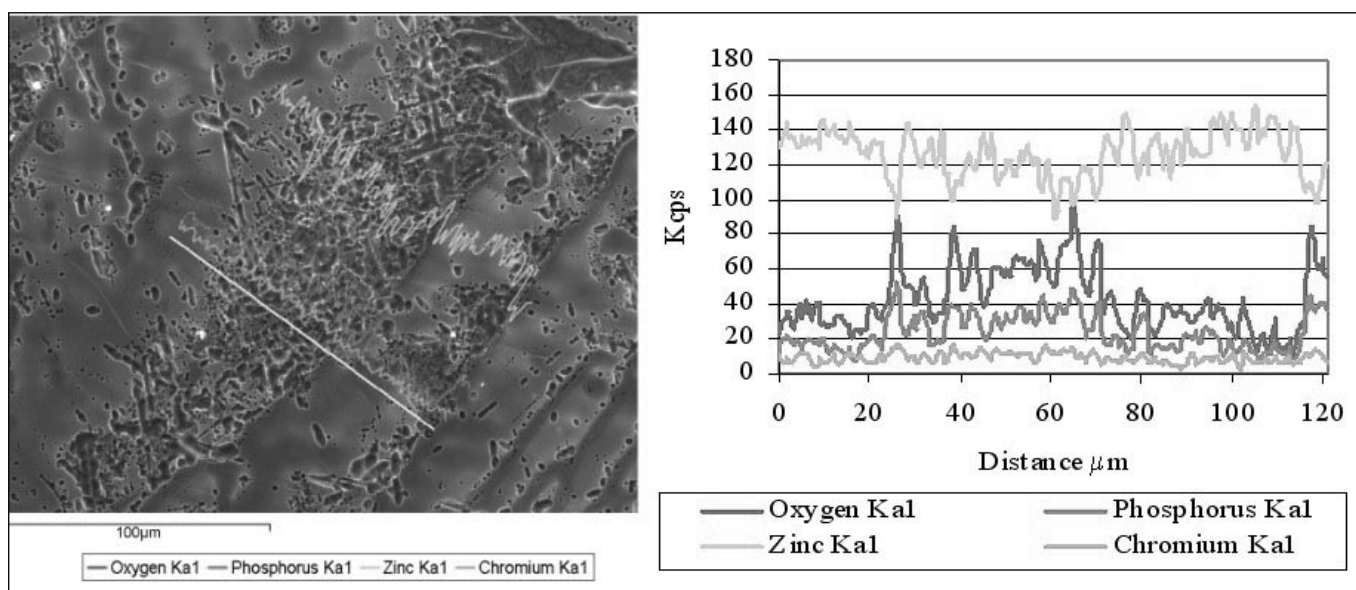


Fig. 8 – SEM/SE image of the surface of a G specimen: preferential attack areas are evidenced and porosities concentrations; EDS composition profiles for various elements.

Fig. 8 – Immagini SEM/SE della superficie di un campione G: sono evidenziate aree di attacco preferenziale e porosità; profili di composizione EDS per i vari elementi.

areas are unattached. Only ZP9 sample shows a corrosive attack limited to 20-30% of the overall surface. In any case the attack is localized and it is related to the presence of a thinner passivation layer in some areas where the corrosion starts.

As shown in Table 5 a good relationship between the Cr content and the corrosion behaviour may be established only for sample ZP9 (Cr content 21 mg/m²) with respect to all the other specimens (Cr content 6-10 mg/m²): the test does not allow to discriminate between lower Cr contents.

The G specimens, after 96 h of exposure, show a percentage of the surface corroded of 40-50%, moreover at the end of the test the corrosion attack is localized, due to punctual chromium content variations, as confirmed by EDS analysis.

EDS analysis show a difference in the Cr content from one point to another on the surface of G specimens, starting from the attached areas the corrosion spreads out and covers the all

surface, the corrosion products are mainly constituted by Zn oxychlorides. The protection efficacy increases with increasing the thickness of the coatings. The results listed in Table 5 evidence that the Cr(III) passivation treatment gives a better corrosion resistance than the traditional passivation treatment. Not more than 40-50% of the exposed surface appears corroded on the G samples after 96 h of exposure. It has to be taken into account that chromium content in the passivation layer obtained of ZP specimens is lower than the one of G specimens. As a matter of fact in the former case the Cr content is maintained deliberately low for aesthetic reasons, otherwise the layer darkens.

Electrochemical characterization

In Fig. 9 the Nyquist diagrams recorded on a hot dip galvanized steel sample at increasing immersion times in sodium

Table 5 – Results of the salt spray tests at increasing exposure times expressed as % of corroded surface evaluated by VE (Visual examination) and IA (Image analysis).

Tabella 5 – Risultati del test in nebbia salina, a tempi crescenti di esposizione, espressi come % della superficie corrosa valutata per esame visivo (VE) e per analisi d'immagine (IA).

Code	Cr content (mg/m ²)	Corroded surface (%)				
		VE 24 h	VE 48 h	VE 72 h	VE 96 h	IA 96 h
Z2	-	>80	-	-	-	-
ZP1	7	5÷10	55	>80	-	-
ZP2	6	~70	>80	-	-	-
ZP3	8	~50	80	>80	-	-
ZP4	10	15÷20	50÷60	>80	-	-
ZP5	6	25÷30	80	>80	-	-
ZP6	9	25÷30	60÷70	>80	-	-
ZP7	7	Start	30	60÷70	>80	-
ZP8	8	~10	45	70	>80	-
ZP9	21	0	Start	5÷10	20÷30	-
ZP10	9	Start	35÷40	>80	-	-
G1/a	20	Start	10÷15	15÷20	20	29
G1/b	38	0	Start	5	5÷10	21
G2/a	20	Start	20÷25	25÷30	40÷50	53
G2/b	38	0	Start	5	10	8
G3/a	20	0	5	5÷10	20÷25	14
G3/b	38	0	Start	Start	Start	3

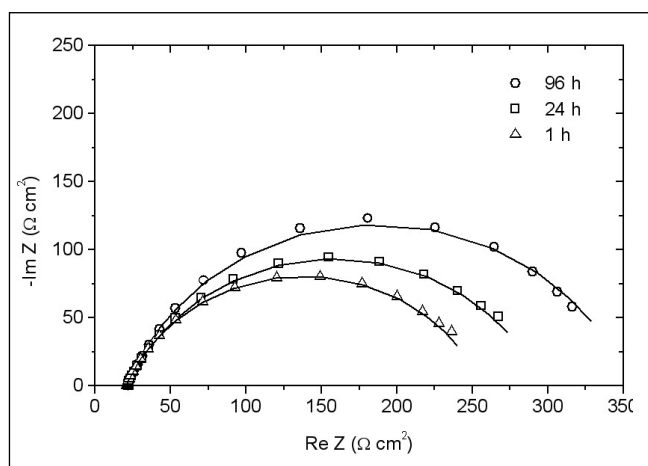


Fig. 9 – Nyquist diagrams recorded on a Z specimen in NaCl 0.1 M aerated solution at increasing immersion periods.

Fig. 9 – Diagrammi di Nyquist ottenuti su un campione Z in soluzione di NaCl 0.1M a tempi crescenti di immersione.

Immersion period (h)	R _{ct} (Ω cm ²)
1	235
24	275
96	330

Table 6 – Charge transfer resistance (R_{ct}) values evaluated by the analysis of the impedance spectra of Fig. 9 recorded in NaCl 0.1 M solution.

Tabella 6 – Resistenza al trasferimento di carica (R_{ct}) valutata dagli spettri di impedenza riportati in Fig. 9 e registrati in soluzione di NaCl 0.1M.

chloride solution are shown. In all cases only one capacitive loop is present and may be attributed to the dissolution of zinc under charge transfer control [11-12]. From the analysis of the impedante spectra [13] the charge transfer resistance, R_{ct}, may be evaluated as shown in Table 6. By increasing the immersion period, an increase of the R_{ct} value is observed and may be attributed to the presence of

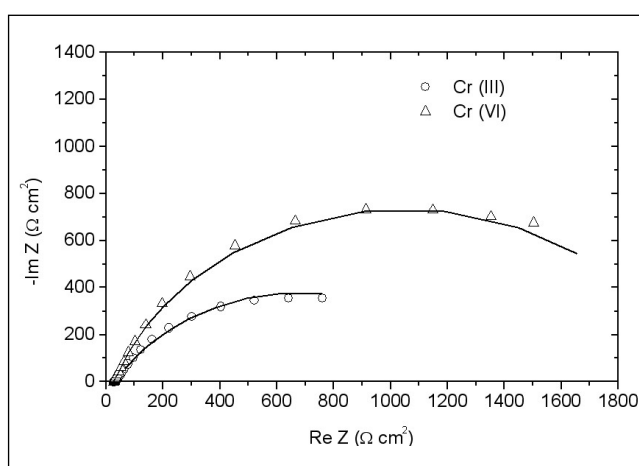


Fig. 10 – Nyquist diagrams recorded on G and ZP specimens in NaCl 0.1 M aerated solution after 1 h of immersion.

Fig. 10 – Diagrammi di Nyquist ottenuti su campioni G e ZP in soluzione di NaCl 0.1M dopo 1 h di immersione.

Code	R _{ct} (Ω cm ²)
ZP6	2100
G3/b	1400

Table 7 – Charge transfer resistance (R_{ct}) values evaluated by the analysis of the impedance spectra of Fig. 10 recorded in NaCl 0.1 M solution after 1 h of immersion.

Tabella 7 – Resistenza al trasferimento di carica (R_{ct}) valutata dagli spettri di impedenza riportati in Fig. 10 e registrati in soluzione di NaCl 0.1M.

corrosion products, mainly Zn oxyhydroxychlorides, as confirmed by the SEM-EDS observation; this layer hinders the further Zn dissolution. Fig. 10 shows the Nyquist diagrams recorded in NaCl 0.1 M solution after 1 h of immersion of the G and ZP specimens submitted to the passivation treatment respectively in chromic acid and with Cr(III).

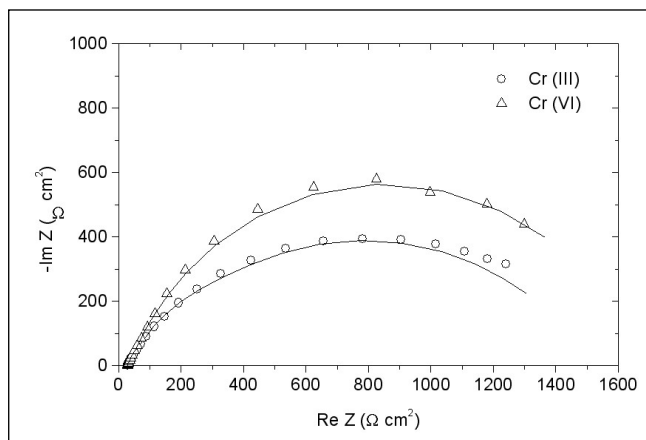


Fig. 11 – Nyquist diagrams recorded on G and ZP specimens in NaCl 0.1 M aerated solution after 24 h of immersion.

Fig. 11 – Diagrammi di Nyquist ottenuti su campioni G e ZP in soluzione di NaCl 0.1M dopo 24 h di immersione.

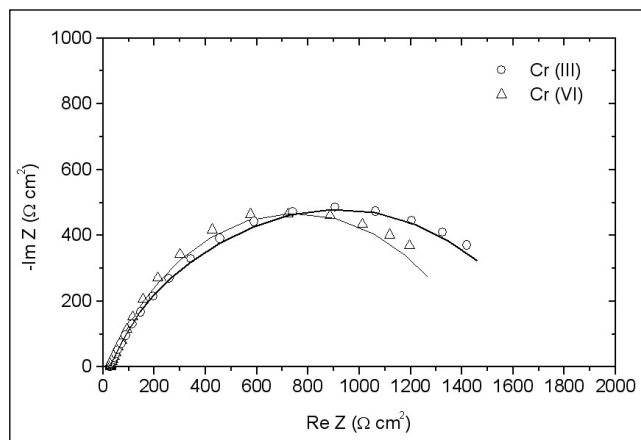


Fig. 12 – Nyquist diagrams recorded on G and ZP specimens in NaCl 0.1 M solution after 96 h of immersion.

Fig. 12 – Diagrammi di Nyquist ottenuti su campioni G e ZP in soluzione di NaCl 0.1M dopo 96 h di immersione.

In this case too the impedance spectra are characterized by the presence of a single capacitive loop, whose amplitude is a function of the passivation treatment performed. In Table 7 the listed R_{ct} values show that the passivation treatment with Cr(III) increases the corrosion resistance of the hot dip galvanized steel because of the barrier action of the insoluble Cr(III) products, essentially chromium oxyhydroxides [14-15] with respect to the aggressive agents (O_2 , Cl⁻).

However, it has to be underlined that the highest reduction of the corrosion rate has been observed with ZP specimens, notwithstanding the lower Cr content in the layer (9 mg/m² with respect to 38 mg/m² of the G samples). The result may be justified taking into account that with chromating, the protective effectiveness is twofold: as barrier effect as in the case of the Cr(III) passivation treatment, as corrosion inhibitor because of the presence of soluble Cr(VI) products [2,16]. At increasing immersion time, an inversion of this tendency may be observed, as well evidenced by the shape of the Nyquist diagrams of Fig. 11 and 12. A decrease of the amplitude of the capacitive loop of the diagram of the ZP specimen, as well evidenced by the R_{ct} values in Table 8.

The decrease of the protective performance, found also by other Authors [17-18], has to be attributed to the low number of Cr(VI) species, responsible of the self-healing effect versus the zinc dissolution [19-20], at disposal. The passivation layers obtained on G samples, having a higher Cr content, show a higher corrosion resistance at increasing immersion times, as shown by the R_{ct} values listed in Table 8.

CONCLUSIONS

From the above-exposed findings a comparison can be made between the protective efficacy of a traditional passivation treatment and an innovative Cr(III)-based passivation treat-

ment on hot dip galvanized steels. The surface of the specimens after the Cr(III) passivation treatment remains shiny and does not change from a visual point of view, differently from what happens with the traditional treatments. The amount of chromium in the layer after treatment with chromic acid is 6-10 mg/m², while the passivation with Cr(III)-based product with the above-mentioned process parameters leads to 20-30 mg/m². The surface morphology is substantially uniform after the traditional process, while the Cr(III) treatment causes a localized attack. The salt spray test, after 24 h exposure, show that the Cr(III)-based passivation treatment has a better protective performance with respect to the traditional chromating treatments, with a lower chromium content. The electrochemical impedance measurements allow to evidence that the Cr(III)-based passivation treatment increases the corrosion resistance of hot dip galvanized steels in chlorides solution for long exposure periods, while the traditional passivation treatment works better for short immersion periods: the different behaviour may be attributed to the different chromium content in the layers and to the inhibiting action of the Cr(VI) species found in the surface passivated with chromic acid.

REFERENCES

- [1] T. Bellezze, G. Roventi, R. Fratesi, Surf. Coat. Technol. 155 (2002) 221
- [2] T. Biestek, J. Weber, Conversion Coatings, Portcullis Press, Redhill, 1976
- [3] M. P. Gigandet, J. Faucheu, M. Tachez, Surf. Coat. Technol. 89 (1997) 285
- [4] X. Zhang, C. van den Bos, W. G. Sloof, A. Hovestad, H. Terryn, J. H. W. De Wit, Surf. Coat. Technol. in press
- [5] W. E. Pocock, Met. Finish. 52 (1954) 48
- [6] E. Akiyama, A. J. Markworth, J. K. McCoy, G. S. Frankel, L. Xia, R. L. McCreery, J. Electrochem. Soc. 150 (2003) B83
- [7] P. C. Wynn, C. V. Bishop, Trans, IMF 79 (2001) B27
- [8] C. Barnes, J. B. Ward, T. S. Sehmbhi, V. E. Carter, Trans. IMF 60 (1982) 45
- [9] ASTM B117 – Salt Spray (Fog) Testing, ASTM, Philadelphia, PA, 1994
- [10] M. Zapponi, A. Quiroga, T. Perez Surface & Coating technology, 122 (1999) 18
- [11] T. Hurlen, K. P. Fischer, J. Electroanal. Chem., 61 (1975), 165
- [12] J. T. Kim, J. Jornè, J. Electrochem. Soc., 127 (1980), 8

Code	R_{ct} (Ω cm ²)	
	24 h	96 h
Z		
ZP6	1650	1450
G3/b	1500	1700

Table 8 – Charge transfer resistance (R_{ct}) values evaluated by the analysis of the impedance spectra of Fig. 11 and 12 recorded in NaCl 0.1 M solution after 24 and 96 h of immersion.

Tabella 8 - Resistenza al trasferimento di carica (R_{ct}) valutata dagli spettri di impedenza riportati in Fig. 11 e 12 e registrati in soluzione di NaCl 0.1M dopo 24 e 96 h di immersione.

- [13] G. W. Walter, Corros. Sci., 26 (1986), 681
 [14] M. Kendig, R. Addison, S. Jeanjaquet, J. Electrochem. Soc., 146 (1999), 4419
 [15] P. McCluskey, Trans. IMF, 74 (1996), 119
 [16] L. Xia, E. Akiyama, G. Frankel, R. McCreery, J. Electrochem. Soc., 147 (2000), 2556
 [17] M. Kendig, S. Jeanjaquet, J. Electrochem. Soc., 149 (2002), B47
 [18] G. O. Ilevbare, J. R. Scully, J. Electrochem. Soc., 148 (2001), B196
 [19] G. Goeminne, H. Terryn, A. Hubin, J. Vereecken, Electrochim. Acta, 47 (2002), 1925
 [20] P. Campestrini, G. Goeminne, H. Terryn, J. Vereecken, J. H. W. de Wit, J. Electrochem. Soc., 151 (2004), B59

A B S T R A C T

CONFRONTO DELLA RESISTENZA ALLA CORROSIONE DI LAMINATI ZINCATI CON STRATI DI CONVERSIONE A BASE DI CR(III) O CON TRADIZIONALI STRATI DI PASSIVAZIONE A BASE DI CR(VI)

Parole chiave: acciaio, corrosione, trattamenti superficiali, microscopia elettronica, tecnologie

Acciai zincati a caldo sono stati sottoposti a trattamenti di passivazione con prodotti industriali a base di Cr(III) e le proprietà degli strati sono state confrontate con quelle degli strati di passivazione ottenuti con prodotti tradizionali a base Cr(VI), trattamento con acido cromico.

La caratterizzazione del substrato e degli strati protettivi è stata effettuata prima e dopo il trattamento di passivazione mediante microscopio ottico (OM) e microscopio elettronico associato a microsonda a dispersione di energia (SEM/EDS). In particolare lo strato di zinco è stato osservato sulla superficie ed in sezione per evidenziarne la possibile difettività.

La quantità di zinco di rivestimento, espressa in g/m², è stata determinata su ciascuna faccia del nastro zincato mediante differenza di peso prima e dopo decapaggio in acido cloridrico. Lo spessore del rivestimento di zinco è stato determinato, su entrambe le superfici del laminato, sia a partire dalla quantità depositata (g/m²) tramite il rapporto densità=massa/volume sia, su sezioni metallografiche, per mezzo dell'analisi d'immagine. Sui laminati sottoposti a passivazione la determinazione dello spessore di cromo (mg/m²) è stata effettuata tramite spettrometria in assorbimento atomico (AAS).

La morfologia del materiale passivato è stata esaminata analogamente a quanto fatto per il materiale solo zincato.

La resistenza a corrosione è stata valutata sia sul laminato solo zincato sia dopo i diversi processi di passivazione mediante prove in nebbia salina sia mediante spettroscopia di impedenza elettrochimica (EIS).

Le prove in nebbia salina sono state condotte in accordo alla norma ASTM B117. Il degrado della superficie è stato visivamente valutato dalla percentuale di superficie ricoperta da ruggine bianca dopo ogni 24 h di esposizione, fino a 96 h di esposizione. La prova si considera terminata quando la percentuale di superficie attaccata è superiore all'80%.

Le misure di impedenza elettrochimica sono state condotte alla temperatura di 25°C in soluzione aerata di NaCl 0.1 M. La superficie dei campioni esposta all'ambiente aggressivo era 13 cm². Gli spettri di impedenza sono stati registrati al potenziale di libera corrosione, applicando un segnale sinusoidale 10 mV in ampiezza e frequenza variabile nell'intervallo 100 kHz ÷ 10 mHz.

In Tabella 1 sono riportati, per i campioni zincati a caldo (Z), i valori della quantità di zinco (g/m²) nel rivestimento. Le superfici appaiono lucide con grani visibili ad occhio nudo, che presentano dimensioni variabili da laminato a laminato, Fig. 1-2. I grani sono di notevoli dimensioni e di forma irregolare; il loro numero per cm² varia da 9 a 46; nessuna relazione è stata trovata tra il contenuto di alliganti, in particolare dell'antimonio, e la taglia dei grani. Si sono notate differenze fra le due facce di uno stesso laminato, suggerendo un'influenza predominante delle variabili di processo (velocità di linea, velocità di raffreddamento, ecc.).

Come riportato in Tabella 3, per i campioni (ZP) passivati con i tradizionali prodotti a base di Cr(VI), la quantità globale di zinco si differenzia in funzione del materiale prodotto; tra le due facce le quantità di zinco variano da 15 a 45 g/m². Lo spessore del rivestimento di zinco calcolato a partire dalla quantità depositata per m² varia da 8.4 a 16.8 µm con una differenza massima fra le due facce pari a 6.3 µm. La quantità di cromo depositata sugli zincati tramite passivazione a base di acido cromico è riportata in Tabella 4 e varia da 5 a 21 mg/m². La quantità depositata è mantenuta bassa per esigenze estetiche e per l'effettiva resistenza a corrosione richiesta per l'uso previsto. Infatti è noto che all'aumentare della quantità di cromo nello strato passivato, utilizzando un trattamento di passivazione di tipo tradizionale, il colore del rivestimento tende ad imbrunire. La superficie dello zincato dopo passivazione conserva la propria lucentezza. All'esame in microscopia ottica non si notano modifiche sostanziali apportate dal processo di passivazione, Fig. 3. Al SEM la superficie passivata appare piuttosto uniforme e in generale priva di difetti, Fig. 4.

I campioni zincati a caldo sono stati sottoposti a trattamento di passivazione con prodotti contenenti Cr(III), in modo da ottenere due diverse quantità di cromo nello strato di passivazione: 20 mg/m² (campioni G1/a, G2/a, G3/a) e 38 mg/m² (campioni G1/b, G2/b, G3/b). La superficie conserva la propria lucentezza e non appare alterata rispetto a quella del laminato solo zincato. Le micrografie SEM, Figg. 5 e 6, mostrano le diverse morfologie dei grani, la segregazione dendritica e l'attacco provocato dal trattamento di passivazione.

Le prove in nebbia salina, Tabella 5, mostrano che il trattamento di passivazione a base cromo trivalente offre una buona protezione alla corrosione dei rivestimenti zincati di produzione industriale tradizionale. A confronto, la resistenza alla prova dei rivestimenti di zinco passivati con acido cromico risulta inferiore; tuttavia il deposito di cromo riscontrato nello strato di passivazione è in questo caso molto minore.

Le misure di impedenza elettrochimica più sensibili, Fig. 9-12, hanno evidenziato che il trattamento di passivazione a base Cr(III) comporta un incremento della resistenza a corrosione di acciai zincati in soluzione di cloruri, in particolare per periodi medio - lunghi di esposizione all'ambiente aggressivo, mentre per tempi brevi la cromatazione risulta più efficace. Il diverso comportamento osservato può essere attribuito al differente tenore in cromo degli strati che si originano in seguito a tali trattamenti, il quale sembra giocare un ruolo importante sull'entità sia dell'effetto barriera esercitato dai composti insolubili del Cr(III) che dell'azione inibitrice esplicata dalle specie a base Cr(VI). In tal caso, la ridotta disponibilità di queste ultime limita nel tempo le proprietà anticorrosive della passivazione con acido cromico, compatibilmente con la specificità dell'applicazione industriale in cui i rivestimenti trovano impiego.

La superficie degli zincati dopo passivazione con il prodotto a base di cromo trivalente conserva la lucentezza ed il colore tipico anche con depositi di cromo elevati, il che può permettere di ottimizzare i parametri di processo in modo da ottenere depositi di cromo caratterizzati dalla maggiore resistenza a corrosione possibile senza venir meno alle esigenze estetiche.